JOURNAL OF GEOPHYSICAL RESEARCH, VOL. 115, C04023, doi:10.1029/2009JC005818, 2010

Hindcast and predictability of sporadic Kuroshio-water intrusion (kyucho in the Bungo Channel) into the shelf and coastal waters

Atsuhiko Isobe,[1] Xinyu Guo,[1] and Hidetaka Takeoka[1]

Received 18 September 2009; revised 20 November 2009; accepted 7 December 2009; published 28 April 2010.

[1] Prerequisite(s) for ocean circulation models capable of hindcasting "*kyucho*" occurrence (a sudden coastal temperature rise induced by Kuroshio frontal waves) in the Bungo Channel, Japan, is investigated using long-term observed temperature and sea level time series, archived hydrographic data, and reanalysis data provided by the Japanese Coastal Ocean Predictability Experiment (JCOPE) group. Anticyclonic mesoscale eddies impinging on the Kuroshio front south of the Bungo Channel enhance the frontal sharpness, frontal wave growth, and activity of kyucho phenomena. A kyucho hindcast is carried out to examine the reliability of a numerical model including realistic anticyclonic eddies propagating south of Japan. The Finite Volume Coastal Ocean Model (FVCOM) for which boundary conditions are given by daily JCOPE2 reanalysis data is adopted in the present study. This numerical model does a reasonable job of hindcasting kyucho occurrence in 2003. It is therefore considered that forecasts of kyucho occurrence up to 2 or 3 months ahead are possible by using the FVCOM in conjunction with JCOPE2 forecast data.

Citation: Isobe, A., X. Guo, and H. Takeoka (2010), Hindcast and predictability of sporadic Kuroshio-water intrusion (kyucho in the Bungo Channel) into the shelf and coastal waters, *J. Geophys. Res.*, *115*, C04023, doi:10.1029/2009JC005818.

1. Introduction

[2] Western boundary currents such as the Kuroshio in the East China Sea are often accompanied by frontal waves (or frontal eddies) on their onshore side because these currents are dynamically unstable along shelf breaks [*Qiu et al.*, 1990; *James et al.*, 1999]. These frontal waves may contribute significantly to biological variability over shelves because growing frontal waves play a key role to uplift offshore nutrient-rich intermediate water onto shallow shelves as shown in the well-known schematic of *Lee et al.* [1981]. In fact, *Isobe and Beardsley* [2006] demonstrate that the onshore volume transport across the East China Sea shelf break is maintained stably in a finely gridded numerical ocean circulation model where unstable Kuroshio frontal waves are computed realistically, and that the stable transport disappears in the absence of sufficiently growing frontal waves in a coarsely gridded model. Furthermore, on the basis of a box model approach to evaluate the nutrient budget over the East China Sea shelf, *Chen and Wang* [1999] show that a major nutrient source is Kuroshio subsurface water transported across the shelf break. Hence, field measurements on shelves to monitor a nutrient (hence, biological) transition after passage of Kuroshio frontal waves have been of particular interests. However, it is difficult to monitor the transition directly because neither locations nor times at which frontal waves grow sufficiently can be predetermined along the East China Sea shelf break with the length *O* (1000 km).

[3] An area south of Japan is free from one of the above difficulties in monitoring the nutrient and biological transitions induced by growing frontal waves. The growth of Kuroshio frontal waves south of Japan causes sporadic Kuroshio water intrusions into the shelf and coastal waters between Shikoku and Kyushu Islands, Japan [*Akiyama and Saitoh*, 1993; *Arai*, 2005], which are called "*kyucho*" by *Takeoka and Yoshimura* [1988], a pioneering work in this Bungo Channel (Figure 1). Figure 2 demonstrates a satellite-derived sea surface temperature (SST) snapshot of a kyucho onset, where part of a growing Kuroshio frontal wave starts to intrude into the Bungo Channel. The occurrence of kyucho, which stands for "sudden stormy currents" in Japanese [*Takeoka et al.*, 2000], results in fishery damages by sudden (within several days) temperature rises harmful to cultured fishes as well as by strong currents that can break fishery nets [*Takeoka and Yoshimura*, 1988]. However, it also provides us with an opportunity to monitor the nutrient and biological transitions induced by growing Kuroshio frontal waves because field measurements can be limited in space to within the narrow Bungo Channel of width about 50 km. In fact, kyucho induced transitions of phytoplankton biomass and/or species have been pointed out in Bungo Channel research [*Koizumi and Kohno*, 1994; *Katano et al.*, 2007; *Hirose et al.*, 2008]. Hence, we are able to predetermine the location where nutrient and biological transitions may occur after the passage of growing frontal waves (i.e., kyucho).

[1] Center for Marine Environmental Studies, Ehime University, Matsuyama, Japan.

0148-0227/10/2009JC005818

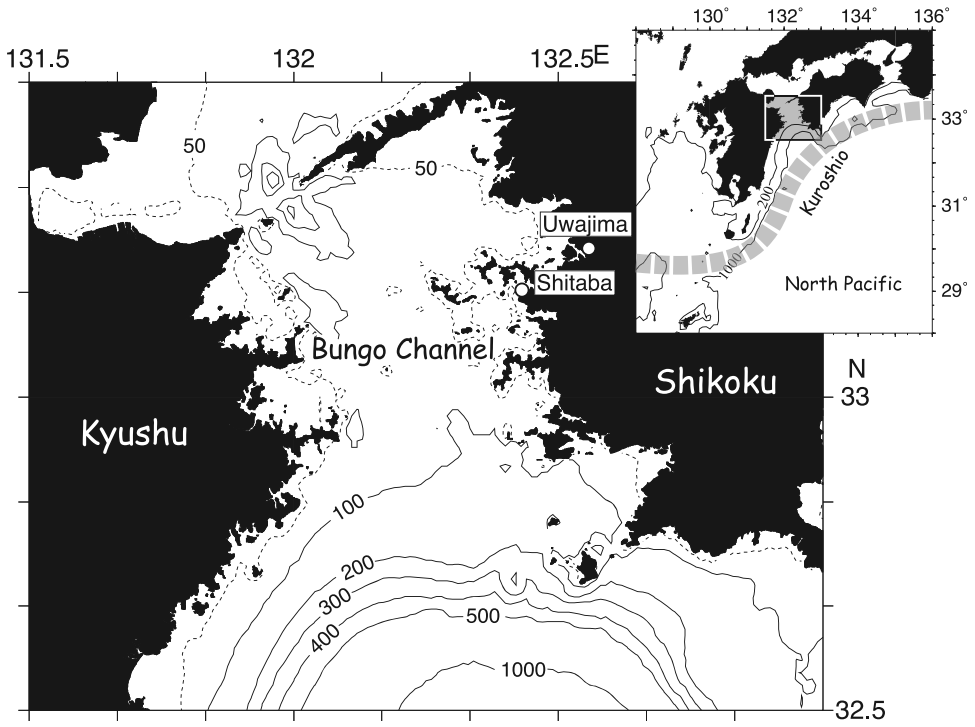

Figure 1. Study area. The area within the square in the inset map is enlarged. The Kuroshio path is shown schematically in the inset map. Also shown are isobaths in meters.

[4] Nevertheless, it is not yet possible to monitor kyucho influences on biological variability over the Bungo Channel because onsets of kyucho need to be predicted before monitoring. The present physical oceanographic study, one part of a research project to elucidate kyucho influences on biological variability over the Bungo Channel, attempts to answer two questions: Is reliable kyucho forecast possible by using a numerical ocean circulation model? What are the prerequisites for a numerical model capable of forecasting the kyucho? First, we address the latter question using long-term observed temperature and sea level time series along the western coast of Shikoku Island, hydrographic data archived in the Japan Oceanographic Data Center (hereinafter, referred to as JODC), and reanalysis data provided by Japanese Coastal Ocean Predictability Experiment (JCOPE2 reanalysis data) [*Miyazawa et al.*, 2008, 2009] group. We thereafter attempt to hindcast kyucho events in a specific year to examine the reliability of the numerical model including the prerequisite(s) detected in the above analyses. The Finite Volume Coastal Ocean Model (FVCOM) [*Chen et al.*, 2003] of which boundary conditions are given by daily JCOPE2 reanalysis data is adopted in the present study. Last, we discuss the predictability of kyucho occurrence using the numerical model available for the kyucho hindcast.

2. Data

[5] An observed temperature record at the Shitaba station (Figure 1) during the period May 2001 through the end of 2007 is analyzed to provide a plausible scenario of kyucho occurrence. A temperature sensor (MDS-MkV/t of JFE-ALEC Co. Ltd) was set at 5 m depth over the course of the above period. Sequential data were subsampled once per hour for the subsequent analyses because various time intervals less than 1 hour were used for the observations. The time series was thereafter band passed using a 5 day Butterworth filter to remove the perturbation induced meteorologically after removal of the seasonal variation by fitting an annual sinusoidal curve.

[6] Tide gauge data at the Uwajima station (Figure 1) are analyzed in conjunction with the above mentioned temperature data because these data might record steric-height variations caused by warm water intrusions during kyucho events. An advantage of tide gauge data is that, in general, a long-term data set is available for analyses; in fact, we use tide gauge data for the years 1967 through 2007 in the present study. Hourly data downloaded on the JODC website (JODC Data Online Service System: http://www.jodc.go.jp) were band passed in the same manner as that for the temperature data. In addition, the inverse barometric effect was compensated for by hourly air-pressure data at the Uwajima meteorological observatory.

[7] In addition to the above two data sets at the fixed stations, temperature data archived for the years 1900 through 2000 were downloaded from the JODC website to investigate climatological temperature patterns south of Japan, which may uncover the plausible scenario for kyucho occurrence. These temperature data at standard depths were converted into 0.5° latitude by 0.5° longitude gridded data using a Gaussian filter with an e-folding scale of 0.25° and a tail length of 0.5°. Before averaging the data in each cell grid, data that exceed three times the standard deviation from their average value were removed. In addition, any cell grid that has less than 10 data values was omitted. A combination of median and Laplacian filters was used to remove "noisy" patterns after gridding.

[8] Furthermore, using JCOPE2 reanalysis data, we examine a spatiotemporal variation of hydrographic properties

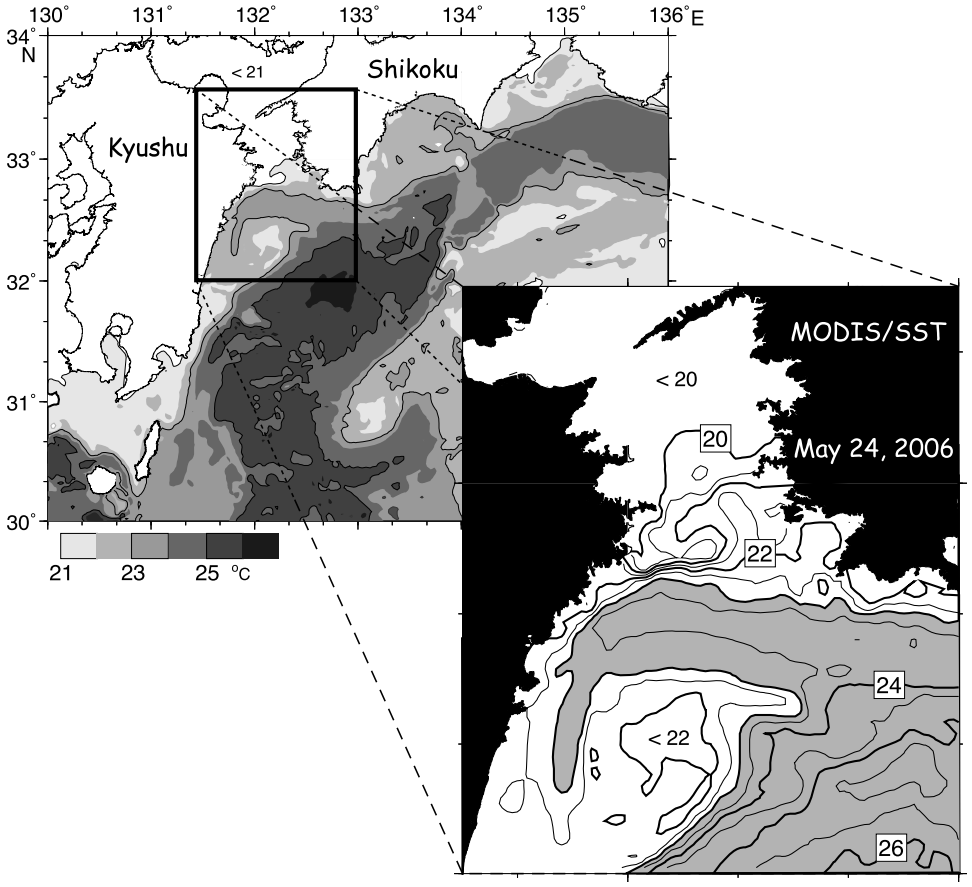

Figure 2. Satellite-derived SST maps in the study area on 24 May 2006. The area within the square is enlarged in the inset. Temperature is indicated by the gray scale at the bottom. The 23°C isotherm line is added to emphasize a folded-wave pattern of a Kuroshio frontal wave south of the Bungo Channel. Contour interval is 0.5°C in the inset. The area with temperature higher than 23°C is stippled to emphasize the Kuroshio frontal wave. The SST data are downloaded on the North Pacific Region Environmental Cooperation Center website (http://www.npec.or.jp/).

south of Japan during the period with intense kyucho events. The JCOPE2 reanalysis data are generated by using a general ocean circulation model to which satellite-derived sea surface height anomalies, satellite-derived SST, and vertical profile data of temperature and salinity obtained from the Global Temperature-Salinity Profile Program are assimilated [*Miyazawa et al.*, 2008, 2009]. *Miyazawa et al.* [2008] demonstrate that their reanalysis data for the years 2003 through 2004 reproduce well the mesoscale eddies propagated south of Japan and Kuroshio meandering triggered by these eddies. Daily data sets of temperature, salinity, sea surface height, and horizontal currents are used in the present study. Besides seeking kyucho-related phenomena south of Japan, these data are used for boundary and initial conditions in a numerical ocean circulation model to hindcast kyucho events in a specific year. The detailed description of this model is provided later in section 4.

3. Prominent Kyucho-Related Variation in Temperature Records

[9] As in the previous Kuroshio frontal wave studies [*Qiu et al.*, 1990; *James et al.*, 1999; *Isobe and Beardsley*, 2006] and kyucho studies [*Akiyama and Yanagi*, 1984; *Akiyama et al.*, 1987; *Takeoka and Yoshimura*, 1988], kyucho events are detected as short-term (less than 1 month) temperature fluctuations (Figure 3). The growth of Kuroshio frontal waves south of Japan and subsequent kyucho occurrences are observed at the southern end of the Bungo Channel throughout the year [*Akiyama and Yanagi*, 1984; *Akiyama et al.*, 1987], while the appearance of significant short-term fluctuations is limited to the seasons spring through autumn in Figure 3. This is because Kuroshio water cannot reach the northern part of the Bungo Channel over the course of winter due to vertical mixing caused by intense surface cooling [*Takeoka et al.*, 1993]. We therefore investigate the periodicity of the temperature fluctuations using a wavelet analysis [*Torrence and Compo*, 1998] suitable to analyze time series with prominent and sporadic fluctuations.

[10] The wavelet spectra (Figure 4) show that temperature fluctuations appear intensely on two different timescales. One is the period less than about 30 days, the typical timescale of kyucho occurrence as shown in Figure 3. It seems that these kyucho-related temperature fluctuations are revealed only in the seasons spring through autumn, as mentioned above, because the intense winter cooling prevents warm Kuroshio water from moving northward. In addition to this annual variation, fortnightly fluctuations (15 day period indicated by

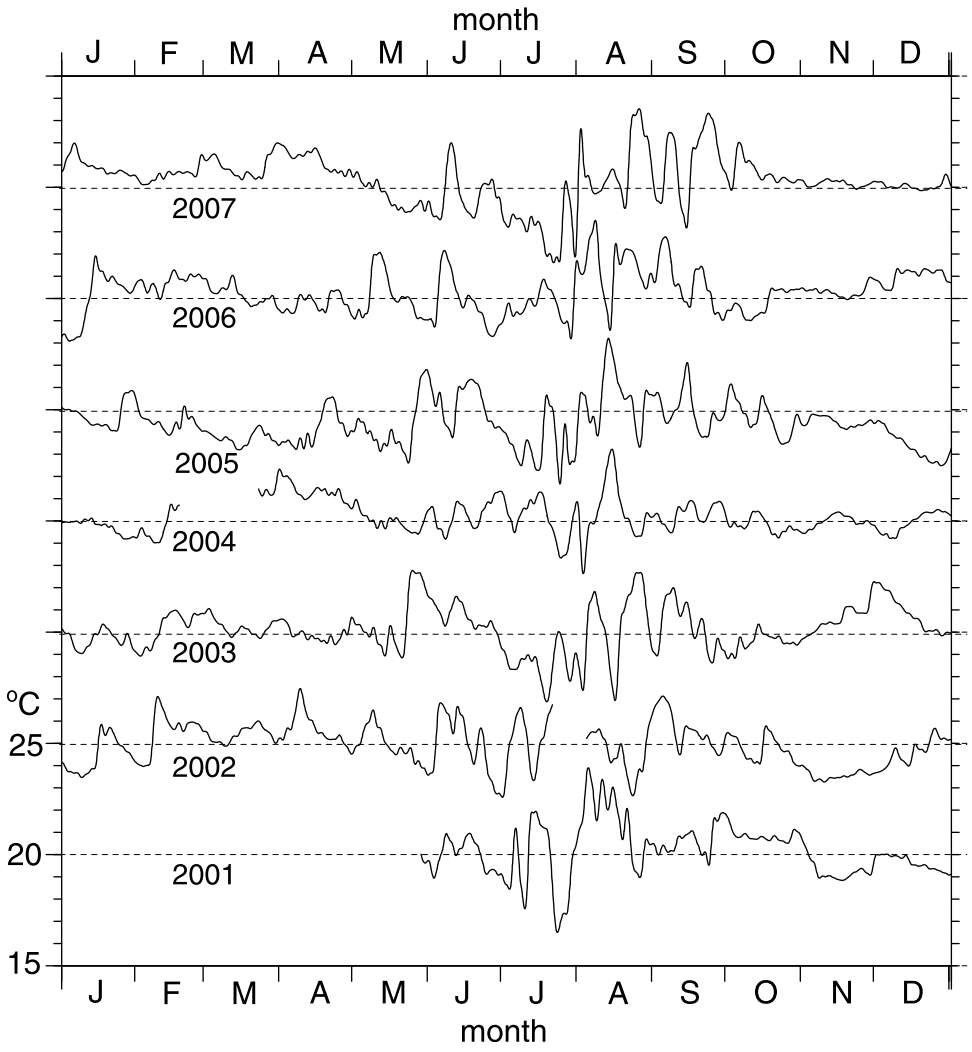

Figure 3. Time series of temperature at the Shitaba station (see Figure 1 for its location) for the years 2001 through 2007. These temperature time series are band passed between 5 days and 1 year. The thin dashed lines indicate the level of 20°C in each year.

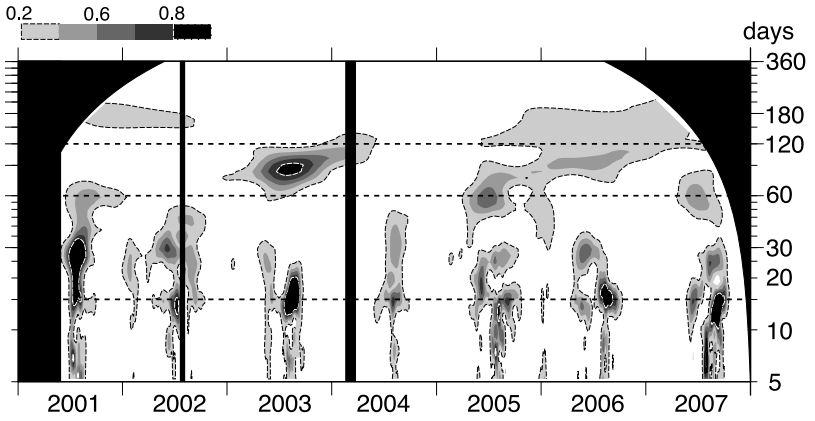

Figure 4. Wavelet spectra for temperature time series from 2001 to 2007. The abscissa represents the time, and the ordinate denotes the period in days. The magnitude of each spectrum is normalized by the variance of that time series, and is indicated by the gray scale shown in the top left. Wavelet spectra cannot be computed on either end because of the finite-length time series [see *Torrence and Compo*, 1998], and so the area is left blank.

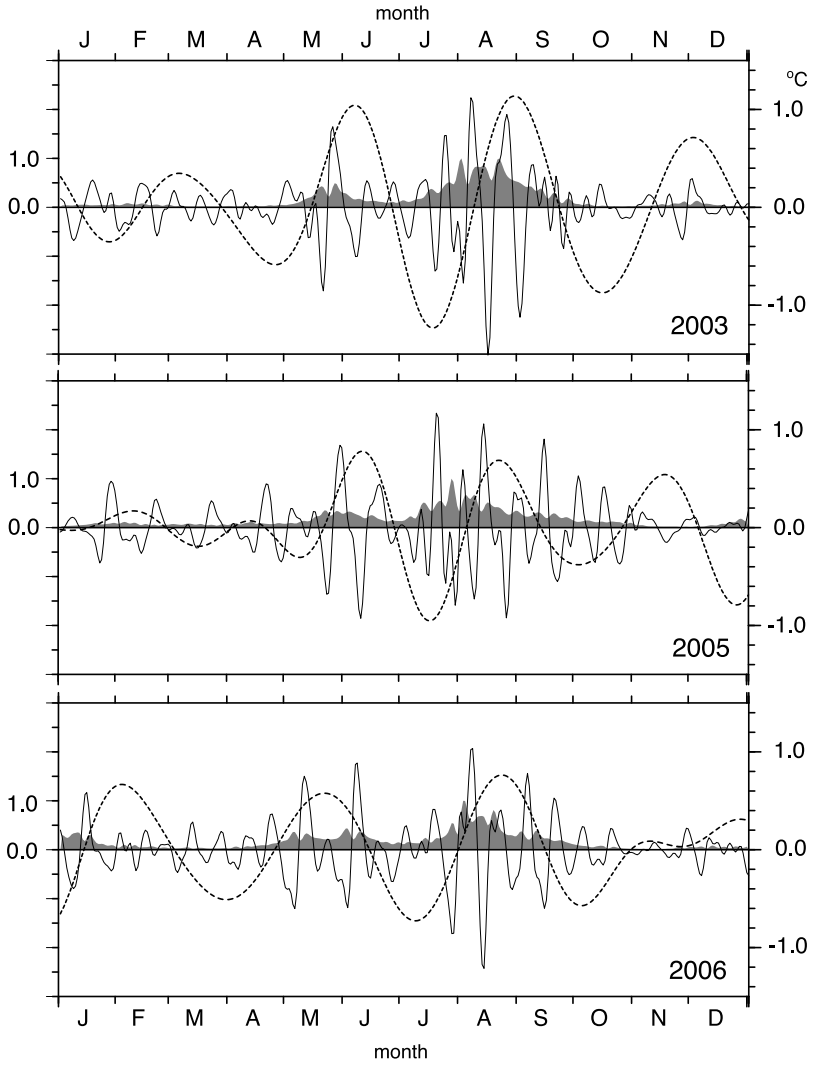

Figure 5. Temperature time series band passed between 5 and 30 days (solid line) and between 60 and 120 days (dashed line) in 2003, 2005 and 2006. The stippled areas represent scale-averaged wavelet spectra between 5 and 30 days. The spectra are normalized by the maximum value in each year. See the right (left) ordinate for the band-passed time series of temperature (scale-averaged wavelet spectra).

a dashed line in Figure 4) are present because the strongly stratified situation at neap tides intensifies the northward transport of warm Kuroshio water in the upper layer [*Takeoka et al.*, 1993]. Another remarkable fluctuation is visible in the period longer than 60 days in Figure 4. The wavelet spectra between 60 and 120 days become energetic when the spectra shorter than 30 days take large values (2003, 2005, 2006, and 2007). On the other hand, the wavelet spectra with both short (<30 days) and long (>60 days) periods weaken together in 2004.

[11] The synchronicity of the temperature fluctuations with different periods (T) suggests that the long-term fluctuation is also associated with kyucho occurrence, so the phase relationship between these two fluctuations is examined next. The temperature time series in 2003, 2005 and 2006 are decomposed into two band-passed series with short (5 days < T < 30 days) and long (60 days < T < 120 days) periods (Figure 5). These 3 years are chosen because both short-term and long-term fluctuations are clearly visible outside the "cone of influence" [*Torrence and Compo*, 1998] at both ends in Figure 4. Also shown by stippling are scale-averaged wavelet spectra for the short-term fluctuations for ease of reference to show the duration with intense kyucho events. Onsets of the events are detected in May and July of 2003, in May and July of 2005, and in April and July of 2006, respectively. The long-term fluctuations are amplified roughly but not exactly in phase with the amplification of the short-term ones (i.e., intense kyucho events). It is however noted that the phase of the long-term fluctuations is somewhat delayed with respect to the amplification of short-term ones.

[12] Both synchronicity and the phase delay suggest that the long-term temperature fluctuations result from the enhancement of the northward heat transport during kyucho events intensified every several months (i.e., 60 days < T < 120 days). If this is the case, the long-term fluctuation must be detected not only in the temperature data, but also in the tide gauge data because the enhanced horizontal heat transport into the Bungo Channel alters the steric height over this area.

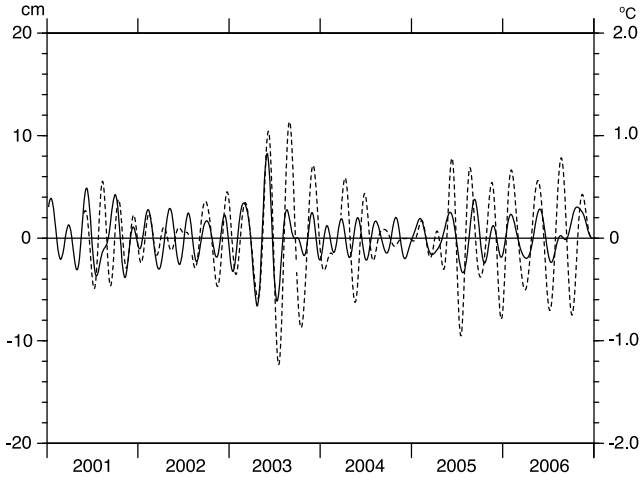

Figure 6. Time series of temperature (solid line; right ordinate) at the Shitaba station and sea level (dashed line; left ordinate) at the Uwajima station. These time series are band passed between 60 and 120 days.

A significant correlation is indeed detected between band-passed temperature data at Shitaba and tide gauge data at Uwajima for the years 2001 through 2006 (Figure 6); the correlation coefficient is estimated to 0.53, a significant value suggested by the *t* test with 99% confidence level.

4. Discussion

4.1. Process by Which Kyucho Occurrence Is Triggered

[13] The activity of kyucho phenomena is enhanced every 60–120 days, and so it is reasonable to consider that a favorable condition of baroclinic and barotropic instabilities leading to the growth of Kuroshio frontal waves occurs south of Japan with a similar period. Climatological temperature patterns south of Japan are next investigated to elucidate the conditions favorable for kyucho occurrence. Figure 7 graphs the tide gauge data band passed between 60 and 120 days for the years 1967 through 2007 at the Uwajima station. As suggested in Figure 6, this long-term fluctuation is anticipated to be significantly correlated with the long-term temperature fluctuation over the course of 41 years. In addition, as suggested by Figure 5, kyucho phenomena are likely to prevail during the periods with large positive values in Figure 7. Figure 8 indicates temperature cross sections along the 132° 20′ longitude; temperature data obtained in the periods when positive (negative) sea level anomalies in Figure 7 are larger (smaller) than the standard deviation are used to define the top left (bottom left) of Figure 8. Figure 8 (top left) shows that an anticyclonic mesoscale eddy is located at 32°N close to the Kuroshio front (32° 30′) when kyucho phenomena prevail in the Bungo Channel, while Figure 8 (bottom left) shows that the anticyclonic eddy mostly disappears when the number of kyucho events decreases.

[14] The relationship between kyucho phenomena and anticyclonic eddies is clarified by investigating anticyclonic eddy behavior south of Japan using the JCOPE2 reanalysis data. In Figure 9 sea surface height anomaly maps are viewed during the period 15 March through 15 May (the former period in Figure 9 (top)), and 15 June through 1 August (the latter period). In the course of the former period, an anticyclonic eddy (positive anomalous area indicated by the letter *A*) far south of Japan on 15 March gradually moves northward (15 April and 1 May), and thereafter impinges on Shikoku Island on 15 May. This anticyclonic eddy *A* remains south of Shikoku Island over the course of the latter period. In addition, another anticyclonic eddy indicated by the letter *B* appears in the study area on 15 June, and thereafter moves northwestward on 1 July. This eddy *B* merges into eddy *A* on 15 July, and it seems likely that eddy *A* strengthens south of Shikoku Island on 1 August. Explicitly, the Kuroshio-front sharpness increases south of the Bungo Channel at the end of both periods (15 May, and 1 August). Special attention should be paid to the fact that the scale-averaged wavelet spectrum (Figure 9 (top)) indicating the activity of kyucho phenomena reaches a peak when the frontal sharpness increases along the northern edge of eddy *A*.

[15] The relationship between anticyclonic eddies south of Japan and kyucho provides us with a scenario to explain how intense kyucho events occur. In general, the increase of frontal sharpness leads to the rapid growth of Kuroshio frontal waves caused by a hybrid of baroclinic and barotropic instabilities [*Qiu et al.*, 1990; *James et al.*, 1999]. It is therefore plausible that anticyclonic mesoscale eddies impinging on the Kuroshio front result in the amplification of frontal waves and an increase of kyucho occurrence in the Bungo Channel. A timescale between 45 and 180 days is taken for mesoscale eddies to pass by a fixed point in the Kuroshio recirculation region south and/or southeast of Japan [*Ebuchi and Hanawa*, 2000]. In particular, using altimeter data, *Ebuchi and Hanawa* [2003] detect anticyclonic eddies carried in the clockwise direction in the region south of Shikoku Island. Based on a center position vector analysis for these eddies, they obtain a rotary spectrum with one peak between 50 and 100 days and another peak on 160 days (see their Figure 9); although their attention is placed on the latter peak, this quasi semiannual spectral peak is unlikely to appear in kyucho phenomena in the Bungo Channel because intense

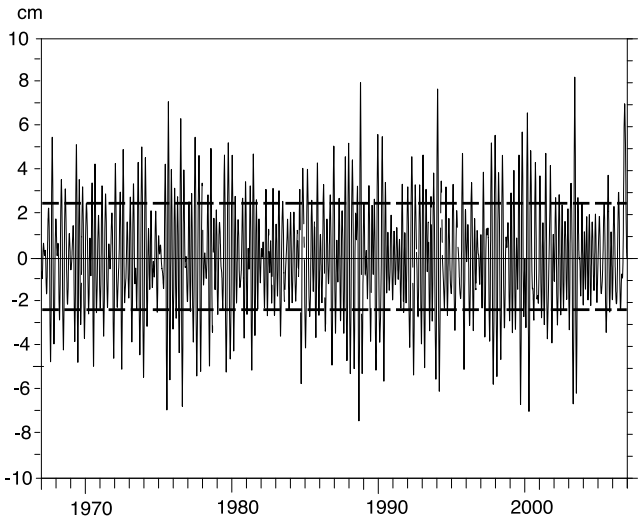

Figure 7. Time series of the sea level at the Uwajima station for the years 1967 through 2007. This time series is band passed between 60 and 120 days. Two dashed lines indicate the standard deviation.

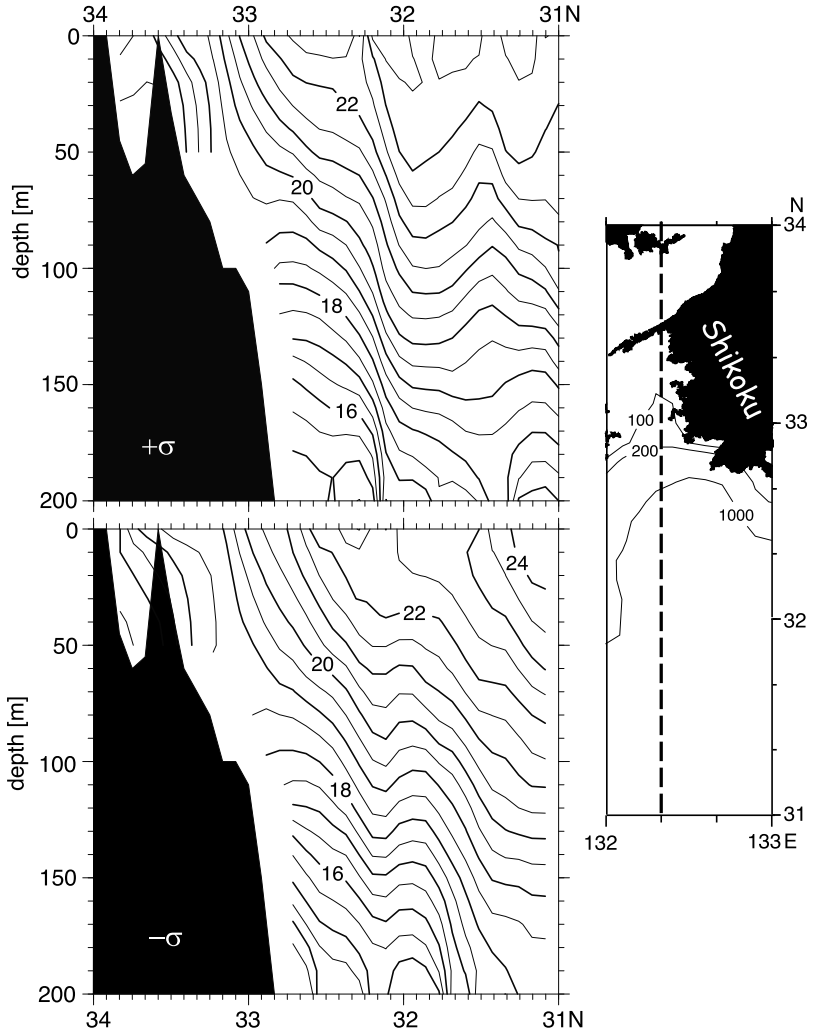

Figure 8. (top left and bottom left) Cross sections of climatological temperature along the dashed line in Figure 8 (right). Temperature data obtained in the years when the sea level is higher (lower) than the positive (negative) standard deviation in Figure 7 are used to depict Figure 8 top left (bottom left). In Figure 8 (left), contour interval is 0.5°C. (right) Also shown are isobaths in meters.

cooling prevents Kuroshio water from moving northward on the winter shelf. The several month timescale with respect to the anticyclonic eddies south of Japan is consistent with that of the intense kyucho events in the Bungo Channel.

[16] The JCOPE2 data reproducing realistic eddy motion may give us a straightforward hindcast method of kyucho occurrence in the Bungo Channel. We next compute the growth rate of baroclinic-instability waves using an Eady's model (Appendix A) applied to daily JCOPE2 data along the line in the 15 March panel of Figure 9. The growth rate is possibly a good index for examining whether or not instability waves (i.e., kyucho) develop at each location along the line; the rate computed in this simple model is mostly determined by the horizontal density gradient, that is, the vertical shear of currents. The growth rate (stippling) is superimposed on the space-time plot of temperature anomaly (contour map) at 100 m depth in Figure 10 (bottom). The area with high growth rates moves northwestward as the anticyclonic eddies approach Shikoku Island for the period March through August (see Figure 9 for eddy motion). It is worth mentioning that the kyucho phenomena prevail in the period May through August (Figure 10 (top), the same one as Figure 5) when the growth rate around Shikoku Island (around 0 km location in Figure 10 (bottom)) remains high. Thus, the growth rate computed in the linear stability analysis using JCOPE2 data is an indicator for kyucho occurrence.

[17] Nevertheless, the growth rate computed in the above procedure is incapable of accurate kyucho hindcasts (hence, forecasts). The time series of the growth rate nearest to Shikoku Island (dashed curve in Figure 10 (middle)) indeed indicates the kyucho event in May. However, the growth rate takes relatively low values for the months July through September over which the kyucho events prevail, presumably because the actual growth rate of kyucho phenomena (i.e., Kuroshio frontal waves) is determined by a complex combination of frontal sharpness, distance between the Kuroshio axis and shelf break, horizontal shear of currents, and so forth [*James et al.*, 1999]. Probably the most reliable method that should be taken for practical kyucho hindcasts/forecasts is the numerical model approach.

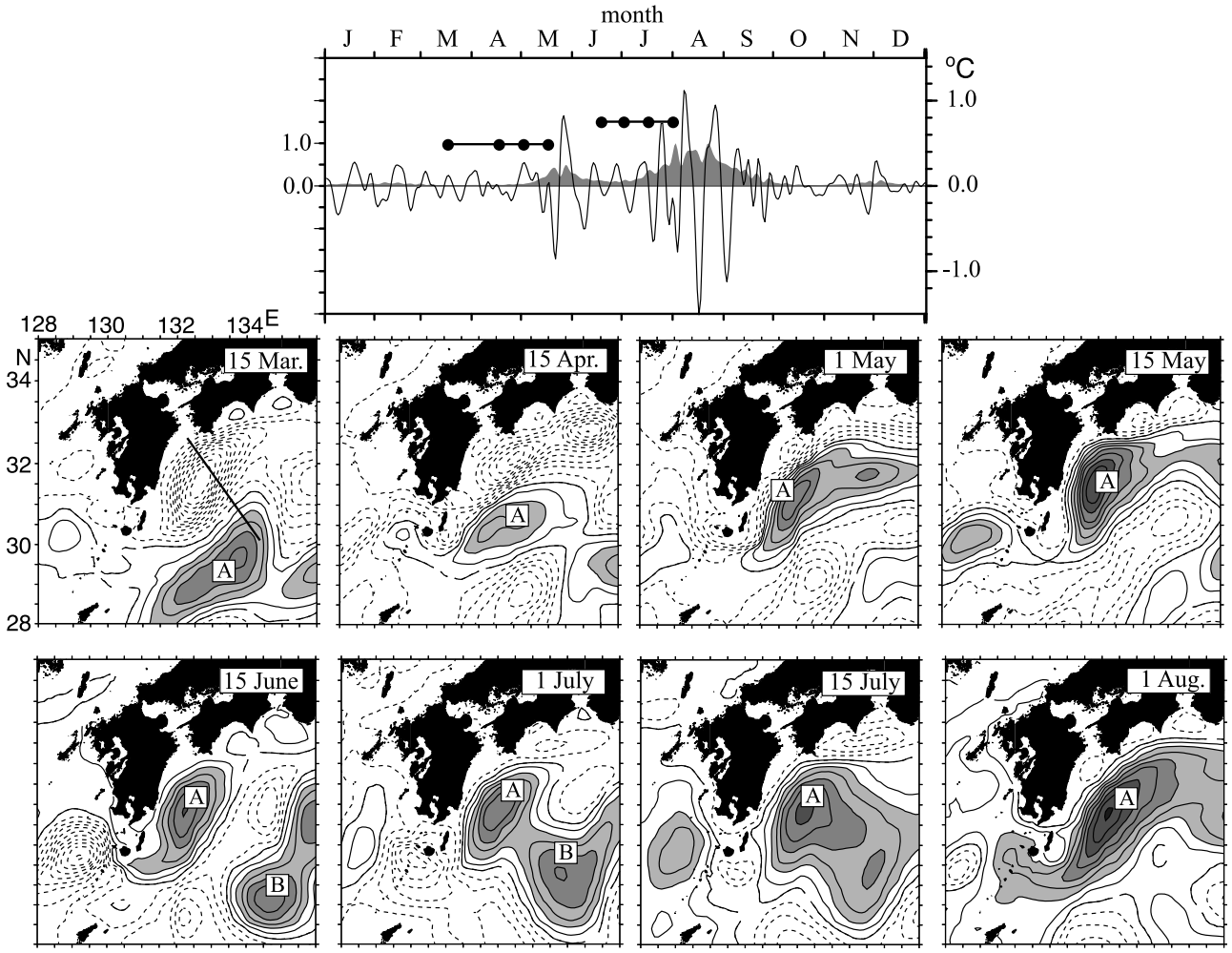

Figure 9. Horizontal distribution of the JCOPE2-provided sea surface height anomaly (middle) from 15 March to 15 May and (bottom) from 15 June to 1 August. The dashed lines are used for negative values. Contour interval is 5 cm. The areas higher than 10 cm are stippled to emphasize anticyclonic eddies. (top) The same as Figure 5 (top) except for eight dots representing the dates shown in the below anomaly maps. The line in the 15 March map is used for Figure 10.

[18] The above discussion provides two prerequisites for the development of a numerical model to hindcast kyucho occurrence. One is the high reproducibility of anticyclonic mesoscale eddies propagated south of Japan because intense kyucho events are triggered by these eddies every several months. For instance, JCOPE2 reanalysis data reproduce well the anticyclonic eddy behavior [*Miyazawa et al.*, 2008] as shown in Figure 9. JCOPE2 data using relatively coarse grids (1/12 degree) are however unsuitable for coastal waters, and so kyucho phenomena are unlikely to be reproduced in the Bungo Channel (~50 km; shown later in Figure 14). Hence, another requirement is a fine resolution that allows us to compute realistically the ocean circulation inside the narrow channel.

4.2. Hindcast of Kyucho Occurrence

4.2.1. Model Description

[19] We next attempt to reproduce kyucho phenomena in a specified year to examine whether or not a numerical model is capable of kyucho hindcasts. Mesoscale eddies, which are approximately a few hundred km in diameter, should be reproduced appropriately over the broad model domain south of Japan, while the model resolution should be sufficiently fine to compute the ocean circulation in the narrow Bungo Channel. Hence, to overcome this difficulty, it is reasonable to adopt the FVCOM with unstructured triangle cell grids to resolve a complex coastal topography using the daily JCOPE2 reanalysis data for the initial and boundary conditions, which are anticipated to introduce mesoscale eddies into the FVCOM domain. These eddies propagated in the model domain enhance the Kuroshio-front sharpness south of the Bungo Channel when they impinge on the front. The fine resolution of the FVCOM has the advantage of realistically computing the growth of frontal waves (hence, kyucho occurrence).

[20] The details for the FVCOM in the present application are described below. We refer the readers to the work of *Miyazawa et al.* [2008] and *Miyazawa et al.* [2009] for details of the JCOPE2 model. Figure 11 demonstrates the model domain along with an enlarged map of unstructured triangle cell grids in the FVCOM. The grid size is set to 9 km at lateral boundaries to connect smoothly with the JCOPE2 data using 1/12 degree structured cell grids in both latitude and longi-

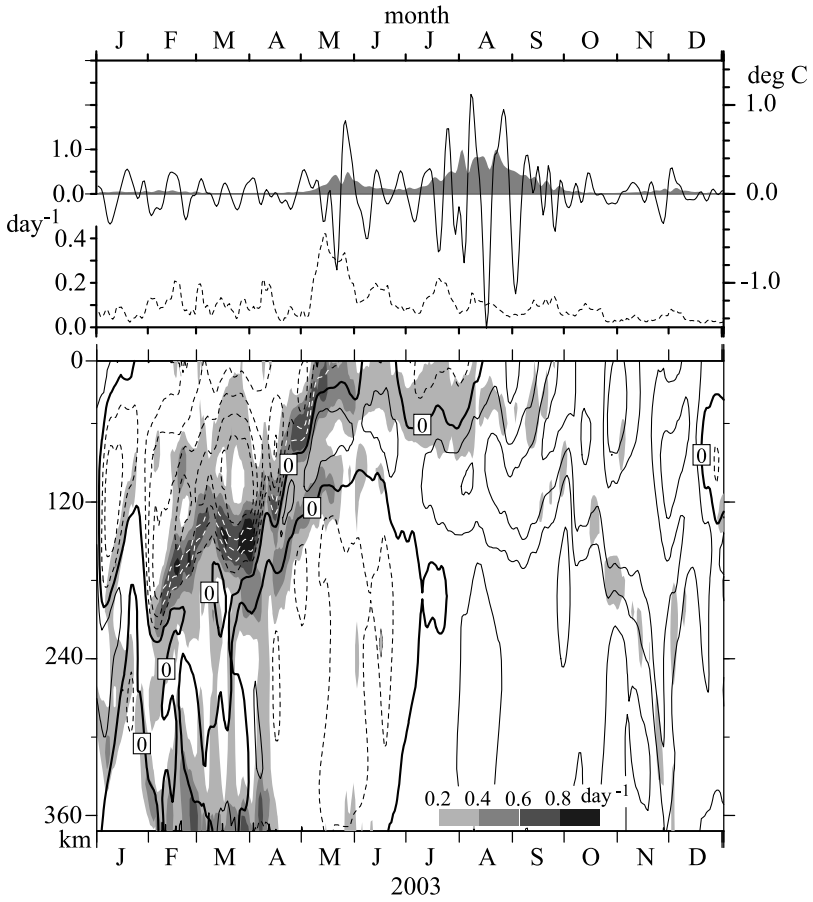

Figure 10. Maximum growth rate computed using an Eady's model with bottom slope applied to year 2003 daily JCOPE2 data along the line in 15 March map of Figure 9 (middle). (bottom) A contour map denoting the space-time plot of temperature at 100 m depth. The ordinate indicates the distance from the northernmost grid. The temperature anomaly from the annual mean at each location is depicted in this panel; the dashed lines are used for negative values. Stippling in Figure 10 (bottom) indicates the growth rate (see Appendix A) of which scale is shown in the lower portion. (top) The same as Figure 5 (top) except for omitting the long-term fluctuations. (middle) The dashed line shows the growth rate at the northernmost grid (x = 0 km) in Figure 10 (bottom).

tude, and diminishes down to 1 km or less in the channel to resolve the complex coastal geometry. Although the FVCOM is a σ coordinate model like the JCOPE2 model with 45 σ layers, the layer number is reduced to 25 in the present application because numerical models are likely to become computationally unstable when the layer thickness is too thin in shallow coastal waters. The topographic data set with a 1/12 degree resolution (ETOPO5) provided by the U.S. National Geophysical Data Center is used for the area south of 31.5°N, while the 500 m gridded topographic data set provided by the Marine Information Research Center, Japan, is used for the area north of 31°N. The depth at each triangle cell grid is given by an interpolation using the nearest 16 topographic data weighted by the inverse distance. The above two topographic data sets are blended to interpolate depths in the area between 31°N and 31.5°N latitudes.

[21] The boundary and initial conditions for the FVCOM are as follows. The horizontal currents, temperature, salinity, and sea level heights in the daily JCOPE2 reanalysis data are given at lateral open boundaries from 15 March 2003 to 30 September 2003. These data sets on 15 March 2003 are used for the initial condition as well. To incorporate JCOPE2-derived variables (f_{JCOPE}) into FVCOM ones (f_{FVCOM}) smoothly, a relaxation scheme, $\alpha(f_{\mathrm{JCOPE}}-f_{\mathrm{FVCOM}})$, is added to conservation equations. The constant α^{-1} changes linearly from 1 hour at the open boundaries to zero at the end of the sponge layer shown by stippling in Figure 11. In addition, to reduce the initial disturbance, the above relaxation scheme is used over the whole region in the course of the first 5 days. The constant α^{-1} changes linearly from 1 hour at the beginning of the computation to zero on day 5. The year 2003 is chosen for the computation because the kyucho phenomena this year seem to be most prominent among the 7 year observations (see Figures 3 and 4). These data are given to each boundary cell grid using a linear interpolation in both time and space.

[22] The modeled SST over the computation period March through September 2003 is restored on a timescale of 5 days to the monthly averaged SST, which is made using the JCOPE2 reanalysis data for the years 2000 through 2002. The year 2003 data are excluded in making these monthly SST maps so that we are able to examine to what extent kyucho occurrence in this specific year is reproduced using only

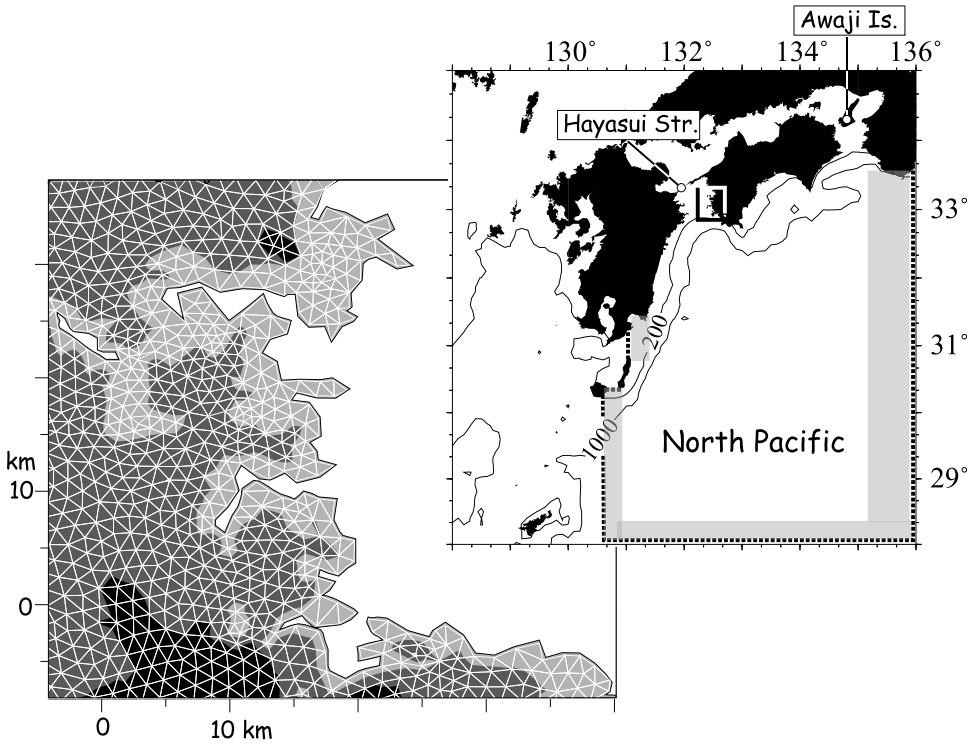

Figure 11. Modeled area using the FVCOM. (right) The bold dashed lines denote the lateral open boundaries of the FVCOM domain. Sidewall boundaries are imposed at Hayasui Strait and Awaji Island. Stippling in indicates "sponge layers" in which FVCOM results are restored to JCOPE2 data to remove artificial disturbances caused by the connection between two different model results. Also shown are 200 and 1000 m isobaths. (left) The area within the rectangle in Figure 11 (right) is enlarged to illustrate unstructured triangle cell grids and depths represented by thin white line and stippling, respectively. Light stippling is used for areas shallower than 50 m, while areas deeper than 100 m are represented by dense stippling.

initial and lateral boundary conditions provided by the JCOPE2 data in the same year. Likewise, other meteorological conditions such as winds and freshwater flux through the sea surface are also omitted in the present application. In addition, tides are excluded from the FVCOM computation as well as the JCOPE2 data because tides are completely predictable, and because the kyucho-favorable condition caused by the weak stratification during neap tides [*Takeoka et al.*, 1993] is also predictable, regardless of which model is used for kyucho hindcasts/forecasts.

4.2.2. Kyucho Occurrence in the Numerical Model

[23] The foregoing analyses show that precise computation of kyucho phenomena in the Bungo Channel requires realistically modeled mesoscale eddies south of Japan, which are revealed due to "release" from the lateral boundaries, existence in the initial field, and generation inside the model domain. The correlation between the sea surface height anomalies in the FVCOM domain and those in the JCOPE2 data indicates that the modeled heights are consistent with the observed field reproduced in the reanalysis data (Figure 12). In fact, Figure 12 shows that the significant values suggested by the *t* test with 99% confidence level are mostly maintained from April 2003 to the end of September although the correlation decreases temporally on 15 May, 30 June, and 20 July. However, it should be noted that the significant correlation disappears in the former half on April. It is therefore considered that eddies in the initial field cannot persist as the computation proceeds, and

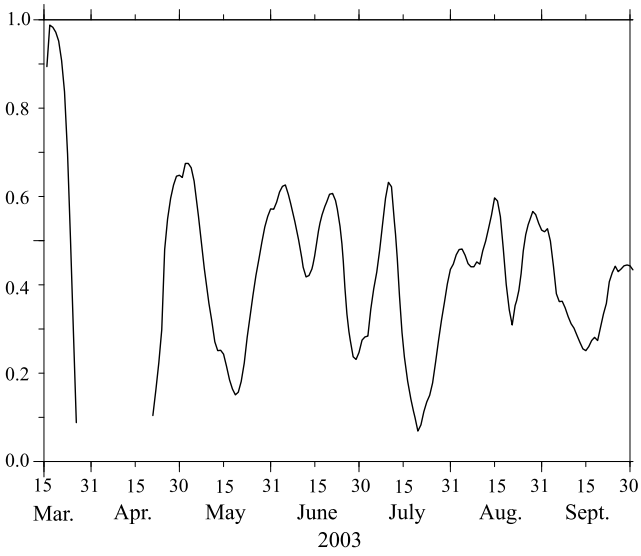

Figure 12. Time series of the correlation coefficient between sea surface height anomalies over the modeled and reanalysis areas deeper than 1000 m depth. The time series is left blank when the coefficient is smaller than a significant value suggested by the *t* test with 99% confidence level.

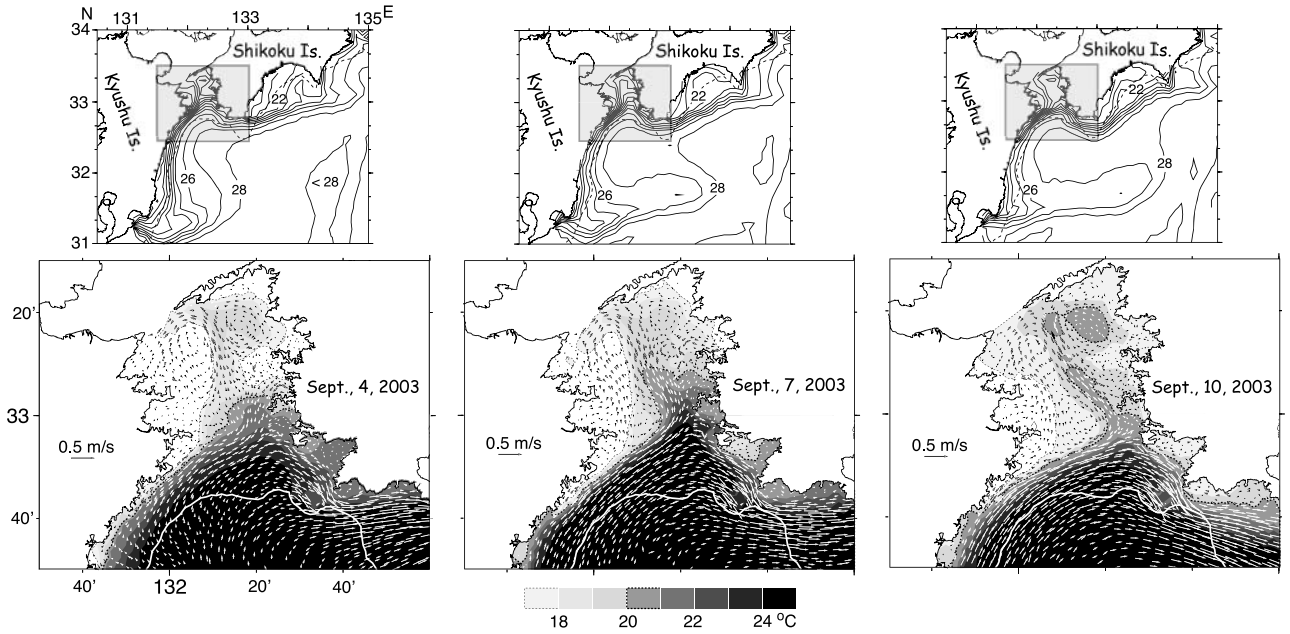

Figure 13. Model results at 5 m depth on 4, 7, and 10 September. (top) The areas within the stippled rectangles are enlarged in Figure 13 (bottom). Figure 13 (top) shows isotherm lines with the interval of 1°C. (bottom) Temperature is indicated by the gray scale shown at the bottom. Note that 20°C isotherms are emphasized using the dashed line. Current vectors are depicted every third cell nodes in Figure 13 (bottom). The 200 m isobath is depicted by the dashed (bold white) line in Figure 13 top (bottom) to indicate the shelf break.

that anticyclonic eddies leading to kyucho occurrence are produced only by release from lateral boundaries and generation inside the model. This disagreement between the modeled and observed fields in April results mainly from the Kuroshio path meandering in the early stage (not shown), presumably due to the growth of disturbances forced at the beginning of the computation.

[24] We next demonstrate how Kuroshio water is carried into the modeled Bungo Channel in the course of a kyucho event. Figure 13 shows temperature and current maps at 5 m depth on 4, 7, and 10 September 2003, respectively. Figure 13 (top) shows that a Kuroshio frontal wave embedded in the Bungo Channel is gradually distorted in the course of 7 days. The 20°C isotherm in the lower enlarged maps indicates more clearly how Kuroshio water is carried onto the shelf in this sporadic kyucho event. The kyucho onset can be seen on 4 September. Thereafter, part of Kuroshio water is carried northward on 7 September when the Kuroshio frontal wave is distorted because Shikoku Island prevents the frontal wave from being propagated eastward (Figure 13 (top)). On 10 September, part of the Kuroshio water is shed from the Kuroshio mainstream south of the Bungo Channel, and moves further to the north in the channel. It is noted that, like the 20°C isotherm in the satellite-derived SST snapshot (Figure 2), the modeled 20°C isotherm extends northward at the central portion in the Bungo Channel on days 7 and 10 September. The kyucho studies to date [e.g., *Takeoka et al.*, 1993], on the basis of the temperature record along the western coast of Shikoku Island, state that kyucho phenomena in the Bungo Channel are regarded as a lock exchange flow in the Kelvin wave sense. However, both the observed SST snapshot (Figure 2) and FVCOM-derived SST maps (Figure 13) demonstrate that the sidewall (i.e., Shikoku Island) is not always required for Kuroshio water intrusions into the Bungo Chanel because a kyucho event is able to develop northward as a growing instability wave. In fact, various satellite images shown by *Akiyama and Saitoh* [1993] also demonstrate kyucho events free from the sidewall.

[25] The modeled temperature time series at the Shitaba station in the FVCOM domain is consistent with the observed one (Figure 14). The observed time series in Figure 14 (top) shows that the short-term fluctuation (i.e., kyucho events) prevails during two periods indicated by bars with the letters *A* and *B*. The JCOPE2 reanalysis data set in the study area is made using a relatively coarse 1/12 degree grid model, so it is unable to reproduce Kuroshio frontal waves with the spatial scale of 100 km [see *Isobe et al.*, 2004, Figure 10]. Hence, the temperature fluctuation in the reanalysis data (dotted line in Figure 14 (bottom)) is unremarkable over the period March through September. However, in the FVCOM domain for which lateral boundary conditions are provided using the daily JCOPE2 data set, two periods *A* and *B* with intense kyucho events are visible in the modeled time series at the Shitaba station. It is therefore concluded both that the numerical model in the present study is able to reproduce anticyclonic eddies leading to the growth of frontal waves, and that the modeled kyucho phenomena indeed resemble as those in the actual ocean. It is however noted that the periods with intense kyucho events are somewhat delayed with respect to the observed ones. For instance, the onset of the period *B* in Figure 14 (bottom) is delayed by about two weeks compared to that in Figure 14 (top) because of the absence

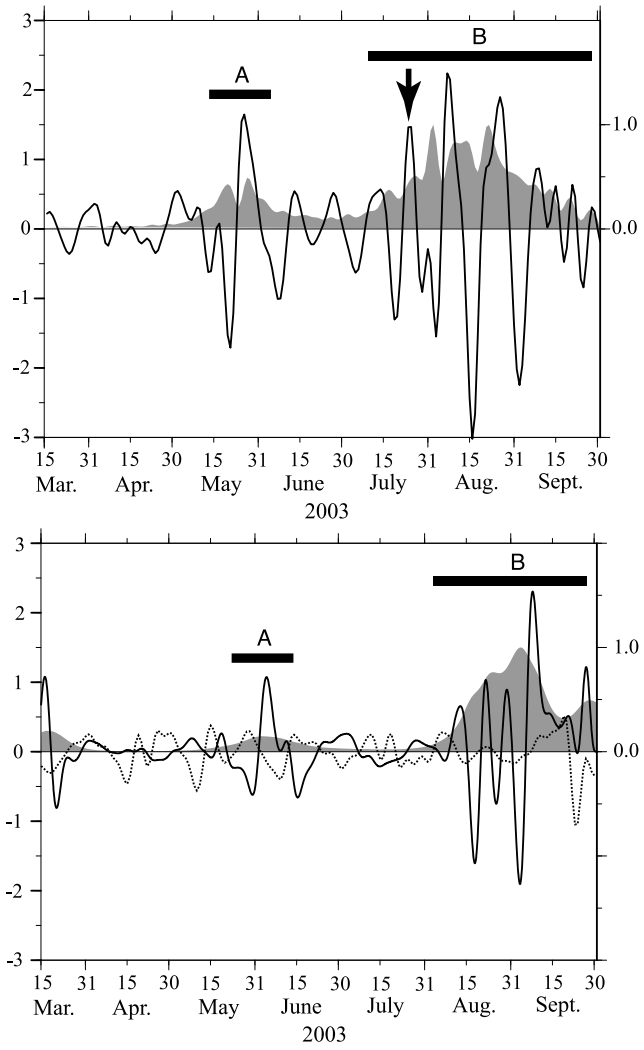

Figure 14. Same as 2003 time series in Figure 5, but for (top) the observed and (bottom) modeled ones at the Shitaba station in the course of FVCOM computation period. The time series in the JCOPE2 reanalysis data is indicated by the dotted line, while the FVCOM results are represented using the solid line. See the text for the meaning of the arrow and bars with letters *A* and *B*.

of the first kyucho event during this period (see the arrow in Figure 14 (top)) in the modeled ocean.

[26] It is unlikely that the absence of winds, freshwater inputs, and tides results in the absence of the first kyucho event in the period *B*. The archived wind data show that moderate (2~3 m/s) winds were maintained south of the Bungo Channel in the latter half of July 2003 (not shown; see Japan Meteorological Agency website, http://www.jma.go.jp), and so the kyucho event is unlikely to be triggered by winds over the actual ocean. Likewise, freshwater supply must not be critical for kyucho occurrence because large rivers are absent from the Bungo Channel. *Takeoka et al.* [1993] indeed point out that kyucho events prevail every neap tidal cycles (weak tidal currents). Nevertheless, the first kyucho event in the period B could not be reproduced in spite of a nontidal model regime in which a kyucho-favorable condition is clearly accomplished. It is therefore reasonable to consider that this kyucho event would not occur even if the numerical model included tides.

5. Conclusion: Is Forecasting of the Kyucho Possible?

[27] The present study has addressed two questions: Is a reliable kyucho forecast possible using a numerical ocean circulation model? What are prerequisites for a numerical model capable of precise kyucho prediction? The answer to the latter question is that well-reproduced anticyclonic mesoscale eddies propagated south of Japan are necessary for the numerical model to enhance the Kuroshio front sharpness south of the Bungo Channel. Were it not for these eddies, the unstable growth of frontal waves (hence, kyucho occurrence) would not appear in the model. In addition, a fine resolution is required for the numerical model to reproduce kyucho phenomena in the narrow (~50 km) Bungo Channel. In the present study, the FVCOM with unstructured triangle cell grids is adopted to compute the ocean circulation using the daily JCOPE2 reanalysis data for the boundary conditions. As shown in Figures 13 and 14, this numerical model does a reasonable job of hindcasting the kyucho occurrence in 2003.

[28] The successful hindcast gives us confidence in the kyucho forecast. It is noted that the present model to hindcast kyucho occurrence is driven only by lateral boundary conditions provided using daily JCOPE2 data in the specific year. The JCOPE2 group is now providing not only reanalysis data, but also forecast data (see their website http://www.jamstec.go.jp/frcgc/jcope/htdocs/distribution/); *Miyazawa et al.* [2005] evaluate the limit of reliable predictability of 50–80 days in forecasting the Kuroshio meander in 1999. Thereby, a forecast system for kyucho occurrence up to 2 or 3 months ahead is possibly established by using the FVCOM in conjunction with JCOPE2 forecast data.

[29] Last, we have to point out a restriction in forecasting kyucho occurrence in terms of the numerical model approach. As shown in Figure 14, the first kyucho event in the period *B* is not revealed in the modeled ocean although two periods during which the number of kyucho occurrences increases can be identified clearly in both observation and model. It is indeed difficult to reproduce the magnitude and/or timing of a single kyucho event accurately because the growth of unstable frontal waves is triggered by small-scale stochastic motion in the actual ocean impossible to compute in models. Therefore, what we are able to forecast in the numerical model approach is not a single kyucho event, but periods during which the number of kyucho occurrences increases. Nevertheless, the onset of these periods may be delayed compared to those in the actual ocean because the first kyucho event in these periods does not always occur in the forecast model. Possibly probabilistic methods such as the ensemble forecast by *Miyazawa et al.* [2005] using JCOPE model will improve the predictability of kyucho events, and will provide a practical forecast system available for kyucho in the Bungo Channel.

Appendix A: Computation of the Growth Rate as an Index of Kyucho Occurrence

[30] The growth rate of baroclinic instability waves in an Eady's model is explained in various text books of geo-

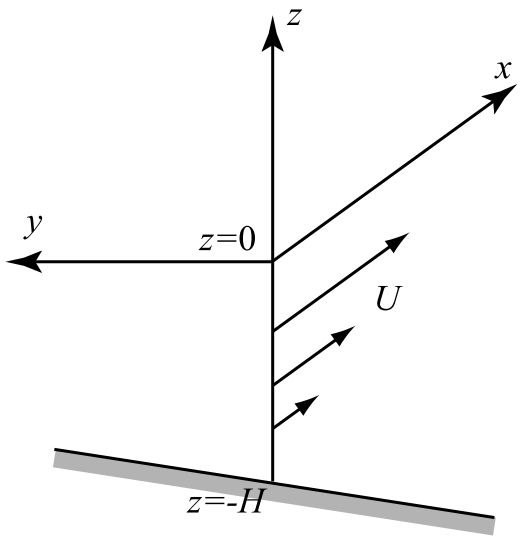

Figure A1. Cartesian coordinate used in the linear stability analysis to compute the growth rate of kyucho around the Bungo Channel. The currents (U) with a linear vertical shear are imposed only in the x direction as shown in this figure.

physical fluid dynamics such as *Cushman-Roisin* [1994], so the essence in computing an index of kyucho occurrence is described below. Let us consider the Cartesian coordinate with a sloping ocean floor (Figure A1). Mean currents (U) are imposed only in the x direction, and have the vertical shear caused by the horizontal density gradient. We start with a conservation equation of the potential vorticity as:

$$(\partial_t + U\partial_x)\left(\nabla^2\psi + f^2N^{-2}\psi_{zz}\right) = 0, \tag{A1}$$

where f, N, ψ are the Coriolis parameter, buoyancy frequency, and stream function for currents ($u = -\psi_y$, $v = \psi_x$) deviated from mean ones, respectively; otherwise the notation is standard. Substituting wavy motion, $\psi = \phi(z)e^{i(kx-\omega t)}$, into equation (A1) yields

$$(\omega - Uk)\left(f^2N^{-2}\phi_{zz} - k^2\phi\right) = 0, \tag{A2}$$

where ω and k denote the frequency and wave number, respectively. A nontrivial solution is readily obtained as:

$$\phi(z) = A\cosh(nz) + B\sinh(nz), \tag{A3}$$

where A and B are constants and n is expressed as kN/f.

[31] As computed in Chapter 15 of Cushman-Roisin's text book, the linearized form of the vertical velocity (w) in quasi-geostrophic dynamics can be written as:

$$w = -fN^{-2}\{\psi_{zt} + J(-Uy, \psi_z) + J(\psi, -U_z y)\}. \tag{A4}$$

Substituting $\psi = \phi(z)e^{i(kx-\omega t)}$ into equation (A4), we obtain

$$w = ie^{i(kx-\omega t)}fN^{-2}\{(\omega - Uk)\phi_z + kU_z\phi\}. \tag{A5}$$

[32] For simplicity, we next introduce a linearized vertical shear of the currents as $U = az + b$. The rigid-lid approximation justifies that the vertical velocity vanished at the surface ($z = 0$), so equation (A5) provides a surface boundary condition as:

$$0 = (\omega - bk)\phi_z + ka\phi. \tag{A6}$$

At the ocean bottom ($z = -H$), vertical velocities generate when the currents in the y component impinge on the bottom slope as:

$$w = \psi_x(-H)_y. \tag{A7}$$

Substituting equation (A7) into w of equation (A5) yields a boundary condition at the ocean bottom as:

$$0 = \{\omega - (b - aH)k\}\phi_z + k\left(a + N^2f^{-1}H_y\right)\phi. \tag{A8}$$

[33] We next substitute equation (A3) into equations (A6) and (A8) to remove the constants A and B, and obtain a quadratic equation with respect to ω as follows:

$$\begin{aligned}\omega^2 &+ k\left\{(aH - 2b) - \theta N^2H\beta_T n^{-1}f^{-2}\right\}\omega \\ &+ (kaH)^2\left[\theta(nH)^{-1}\left\{1 - N^2\beta_T(af)^{-2}\left(a\theta^{-1}n^{-1} - b\right)\right\}\right. \\ &\left.-(nH)^{-2} - b(aH)^{-1} + b^2(aH)^{-2}\right] = 0,\end{aligned} \tag{A9}$$

where β_T ($=fH^{-1}H_y$) denotes the topographic β, and θ is coth (nH). The imaginary part of the solution of equation (A9) gives the growth rate as a function of the wave number (k).

[34] Using daily JCOPE2 density data in the upper 200 m layer, the buoyancy frequency averaged vertically at each grid is computed along the line in the 15 March map of Figure 9. Two coefficients, a and b, representing the vertical structure of currents perpendicular to the line are computed using a least square method by fitting daily JCOPE2 current data in the upper 200 m layer at each grid along the line. The topographic β is given by ETOPO5 depths at neighboring grids along the line. The depth (H) at areas deeper than 200 m is set to 200 m. The maximum growth rate is plotted in Figure 10 by stippling.

[35] **Acknowledgments.** This work is supported by the Japan Society for the Promotion of Science through Grant-in-Aid for Scientific Research (21244073). Comments of two anonymous reviewers and the editor are very helpful in improving the manuscript, and are appreciated.

References

Akiyama, H., and S. Saitoh (1993), The kyucho in Sukumo Bay induced by Kuroshio warm filament intrusion, *J. Oceanogr.*, *49*, 667–682, doi:10.1007/BF02276751.

Akiyama, H., and T. Yanagi (1984), The mechanism of the sudden change of water temperature in Sukumo Bay (in Japanese), *Bull. Coastal Oceanogr.*, *22*, 21–66.

Akiyama, H., T. Yanagi, and K. Nakata (1987), Sudden change of water temperature during summer in Sukumo Bay (in Japanese), *Bull. Coastal Oceanogr.*, *24*, 169–181.

Arai, M. (2005), Numerical study of a kyucho and bottom intrusion in the Bungo Channel, Japan: Disturbances generated by the Kuroshio small meanders, *J. Oceanogr.*, *61*, 953–971, doi:10.1007/s10872-006-0012-3.

Chen, C.-T. A., and S.-L. Wang (1999), Carbon, alkalinity and nutrient budgets on the East China Sea continental shelf, *J. Geophys. Res.*, *104*(C9), 20,675–20,686, doi:10.1029/1999JC900055.

Chen, C., H. Liu, and R. C. Beardsley (2003), An unstructured grid, finite-volume, three-dimensional, primitive equations ocean model: Application to coastal ocean and estuaries, *J. Atmos. Oceanic Technol.*, *20*, 159–186, doi:10.1175/1520-0426(2003)020<0159:AUGFVT>2.0.CO;2.

Cushman-Roisin, B. (1994), *Introduction to Geophysical Fluid Dynamics*, 320 pp., Prentice Hall, Englewood Cliffs, N. J.

Ebuchi, N., and K. Hanawa (2000), Mesoscale eddies observed by TOLEC-ADCP and TOPEX/POSEIDON altimeter in the Kuroshio recirculation region south of Japan, *J. Oceanogr.*, *56*, 43–57, doi:10.1023/A:1011110507628.

Ebuchi, N., and K. Hanawa (2003), Influence of mesoscale eddies on variations of the Kuroshio path south of Japan, *J. Oceanogr.*, *59*, 25–36, doi:10.1023/A:1022856122033.

Hirose, M., T. Katano, Y. Hayami, A. Kaneda, T. Kohama, H. Takeoka, and S. Nakano (2008), Changes in the abundance and composition of picophytoplankton in relation to the occurrence of a kyucho and a bottom intrusion in the Bungo Channel, Japan, *Estuarine Coastal Shelf Sci.*, *76*, 293–303, doi:10.1016/j.ecss.2007.07.030.

Isobe, A., and R. C. Beardsley (2006), An estimate of the cross-frontal transport at the shelf break of the East China Sea with the Finite Volume Coastal Ocean Model, *J. Geophys. Res.*, *111*, C03012, doi:10.1029/2005JC003290.

Isobe, A., E. Fujiwara, P.-H. Chang, K. Sugimatsu, M. Shimizu, T. Matsuno, and A. Manda (2004), Intrusion of less saline shelf water into the Kuroshio subsurface layer in the East China Sea, *J. Oceanogr.*, *60*, 853–863.

James, C., M. Wimbush, and H. Ichikawa (1999), Kuroshio meanders in the East China Sea, *J. Phys. Oceanogr.*, *29*, 259–272, doi:10.1175/1520-0485(1999)029<0259:KMITEC>2.0.CO;2.

Katano, T., et al. (2007), Distribution of prokaryotic picophytoplankton from Seto Inland Sea to the Kuroshio region, with special reference to 'kyucho' events, *Aquat. Microb. Ecol.*, *46*, 191–201, doi:10.3354/ame046191.

Koizumi, Y., and Y. Kohno (1994), An influence of the kyucho on a mechanism of diatom growth in Shitaba Bay in summer (in Japanese), *Bull. Coastal Oceanogr.*, *32*, 81–89.

Lee, T. N., L. P. Atkinson, and R. Legeckis (1981), Observations of a Gulf Stream frontal eddy on the Georgia continental shelf, April 1977, *Deep Sea Res.*, *28*, 347–378, doi:10.1016/0198-0149(81)90004-2.

Miyazawa, Y., S. Yamane, X. Guo, and T. Yamagata (2005), Ensemble forecast of the Kuroshio meandering, *J. Geophys. Res.*, *110*, C10026, doi:10.1029/2004JC002426.

Miyazawa, Y., T. Kagimoto, X. Guo, and H. Sakuma (2008), The Kuroshio large meander formation in 2004 analyzed by an eddy-resolving ocean forecast system, *J. Geophys. Res.*, *113*, C10015, doi:10.1029/2007JC004226.

Miyazawa, Y., R. Zhang, X. Guo, H. Tamura, D. Ambe, J.-S. Lee, A. Okuno, H. Yoshinari, T. Setou, and K. Komatsu (2009), Water mass variability in the western North Pacific detected in a 15-year eddy resolving ocean reanalysis, *J. Oceanogr.*, *65*, 737–756, doi:10.1007/s10872-009-0063-3.

Qiu, B., T. Toda, and N. Imasato (1990), On Kuroshio front fluctuations in the East China Sea using satellite and in situ observational data, *J. Geophys. Res.*, *95*(C10), 18,191–18,204, doi:10.1029/JC095iC10p18191.

Takeoka, H., and T. Yoshimura (1988), The kyucho in Uwajima Bay, *J. Oceanogr.*, *44*, 6–16.

Takeoka, H., H. Akiyama, and T. Kikuchi (1993), The kyucho in the Bungo Channel, Japan—Periodic intrusion of oceanic warm water, *J. Oceanogr.*, *49*, 369–382, doi:10.1007/BF02234954.

Takeoka, H., Y. Koizumi, and A. Kaneda (2000), Year-to-year variation of a kyucho and a bottom intrusion in the Bungo Channel, Japan, in *Interactions Between Estuaries, Coastal Seas and Shelf Seas*, edited by T. Yanagi, pp. 197–215, Terra Sci., Tokyo.

Torrence, C., and G. P. Compo (1998), A practical guide to wavelet analysis, *Bull. Am. Meteorol. Soc.*, *79*, 61–78, doi:10.1175/1520-0477(1998)079<0061:APGTWA>2.0.CO;2.

X. Guo, A. Isobe, and H. Takeoka, Center for Marine Environmental Studies, Ehime University, 2-5, Bunkyo-cho, Matsuyama, 790-8577, Japan. (aisobe@sci.ehime-u.ac.jp)